Strong oxygen participation in the redox governing the structural and electrochemical properties of Na-rich layered oxide Na_2IrO_3

Supporting information

Arnaud J. Perez[1,2], Dmitry Batuk[1,3], Matthieu Saubanère[1,4,5], Gwenaelle Rousse[1,2,4], Dominique Foix[4,6], Eric McCalla[1,4,7], Erik J. Berg[8], Romain Dugas[1,4], Karel H. W. van den Bos[3], Marie-Liesse Doublet[4,5], Danielle Gonbeau[4,6], Artem M. Abakumov[3,9], Gustaaf Van Tendeloo[3] and Jean-Marie Tarascon[1,2,4*]

[1]Collège de France, Chimie du Solide et de l'Energie, UMR 8260, 11 Place Marcelin Berthelot, 75231 Paris Cedex 05, France

[2]Sorbonne Universités - UPMC Univ Paris 06, 4 Place Jussieu, F-75005 Paris, France

[3]EMAT, University of Antwerp, Groenenborgerlaan 171, B-2020 Antwerp, Belgium

[4]Réseau sur le Stockage Electrochimique de l'Energie (RS2E), FR CNRS 3459, 80039 Amiens Cedex France

[5]Institut Charles Gerhardt, UMR 5253, CNRS - Université Montpellier, Place Eugène Bataillon, 34 095 Montpellier, France

[6]IPREM/ECP (UMR 5254), University of Pau, 2 Avenue Pierre Angot, 64053 Pau Cedex 9, France

[7]CEMS, University of Minnesota, 421 Washington Avenue, Minneapolis, Minnesota 55455, United States

[8]Paul Scherrer Institut, Electrochemistry Laboratory, CH-5232 Villigen PSI, Switzerland

[9]Skoltech Center for Electrochemical Energy Storage, Skolkovo Institute of Science and Technology, 143026 Moscow, Russia

* Corresponding author: jean-marie.tarascon@college-de-france.fr

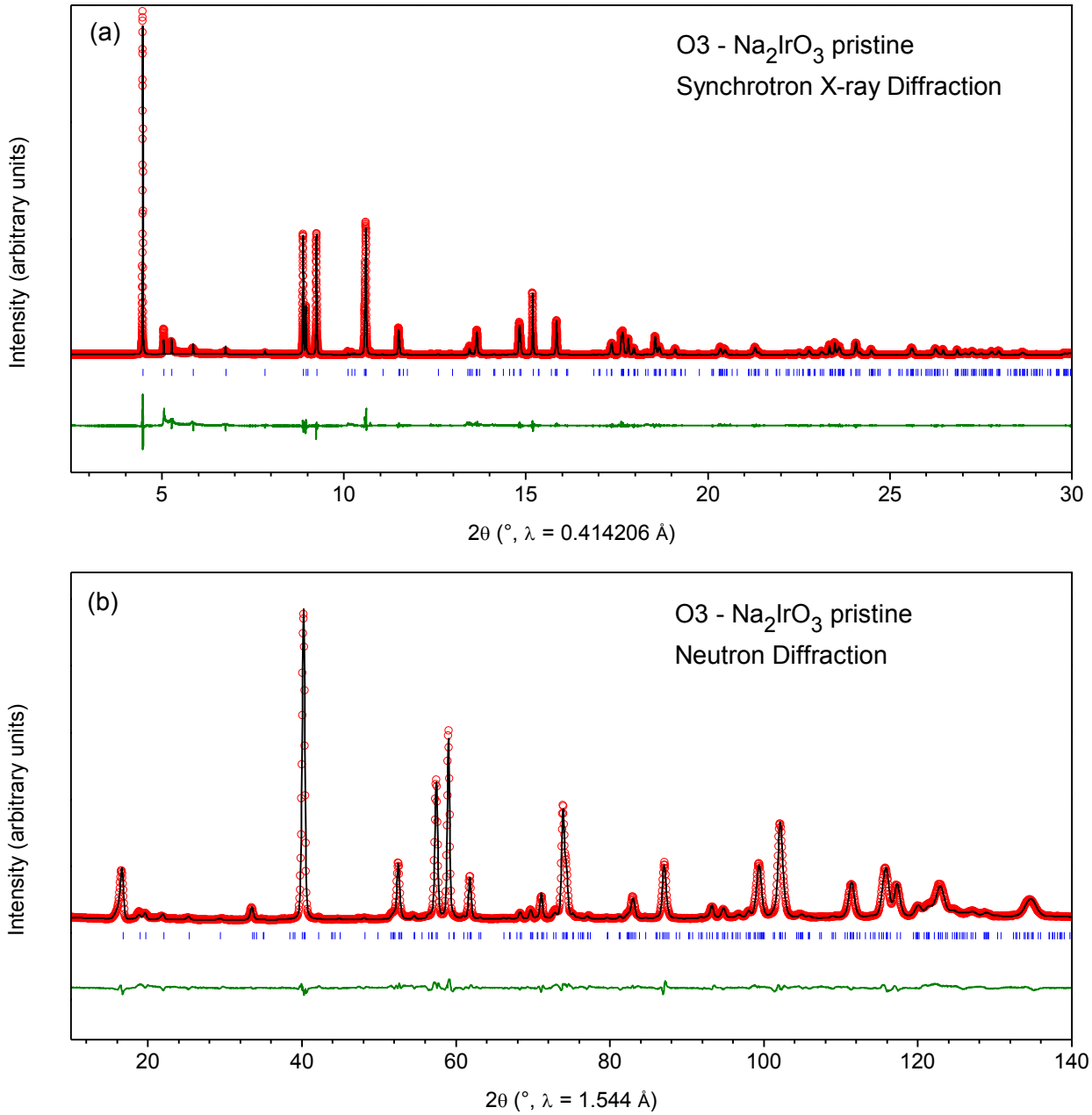

Fig. S1: Rietveld refinement of synchrotron X-ray (a) and neutron (b) diffraction patterns for the pristine Na_2IrO_3 sample. The red circles are the experimental points, the black line is the fit obtained from the Rietveld refinement, the blue ticks are the position of the Bragg reflections and the green line is the difference between the experimental data and the fit. A good fit is obtained for both SXRD and ND data, despite the presence of broad peaks due to stacking faults in the low angle region. Site mixing between Na and Ir in the honeycomb layers (see Table S1) was introduced to artificially reduce the intensity of these peaks in the Rietveld refinement. A better method using the software FAULTS is shown in Fig. S3.

Table S1: Structural parameters for the pristine Na_2IrO_3 sample. Atomic positions were refined from ND data and used as such for the refinement of SXRD data. Some mixing between Ir and Na sites in the honeycomb layer was allowed to artificially reduce the impact of stacking faults on the refinement.

O3 - Na_2IrO_3 pristine

Space group : *C*2/*m*

	a (Å)	b (Å)	c (Å)	β (°)
SXRD	5.42810(3)	9.40318(3)	5.61056(3)	108.9611(5)
ND	5.42698(14)	9.3969(2)	5.60614(10)	108.6371(18)

Atom	Site	x	y	z	Occupancy	B (Å^2)
O1	8j	0.2572(6)	0.3190(3)	0.7944(4)	1	0.13(7)
O2	4i	0.2916(9)	0	0.7934(10)	1	0.78(15)
Ir1	4g	0	0.3339(2)	0	0.878(2)	0.292(8)
Na1	4g	0	0.3339(2)	0	0.122(2)	0.292(8)
Na2	2a	0	0	0	0.756(2)	0.61(3)
Ir2	2a	0	0	0	0.244(2)	0.61(3)
Na3	4h	0	0.8416(7)	0.5	1	0.85(7)
Na4	2d	0	0.5	0.5	1	1.79(15)

Reliability parameters : χ^2 = 6.60, Bragg R-factor = 12.1 % (SXRD)
χ^2 = 18.9, Bragg R-factor = 5.84 % (ND)

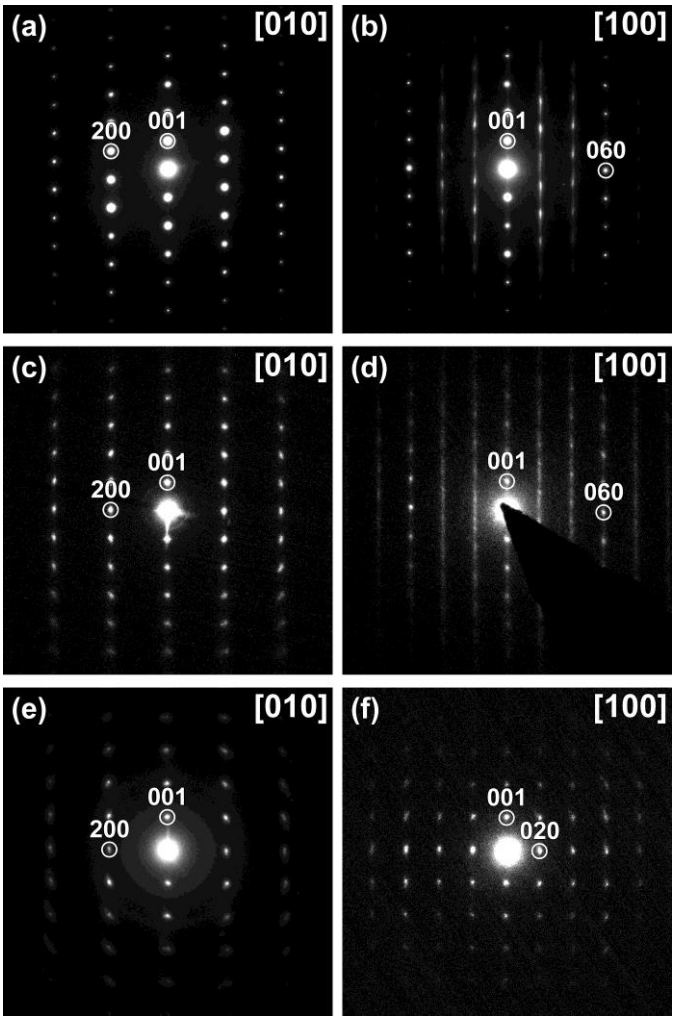

Fig. S2: (a,b) Representative ED patterns for the pristine Na_2IrO_3, indexed on a monoclinic lattice corresponding to the O3 structure. Stacking faults in the structure give rise to the corresponding diffuse intensity in [100] ED pattern, confined to 0*hl*, $h = \pm 2, \pm 4$ reciprocal lattice rows, while reflections in the 0*hl*, $h = \pm 6$ remain sharp. (c,d) ED patterns for the intermediately charge sample to 3 V. The indexes are given with respect to O1 lattice, $a \approx 5.2$ Å, $b \approx 9.1$ Å, $c \approx 4.9$ Å and $\beta \approx 90°$. Note the diffraction intensity streaks due to numerous stacking faults in the arrangement. (e,f) ED patterns for the completely charged sample to 4 V

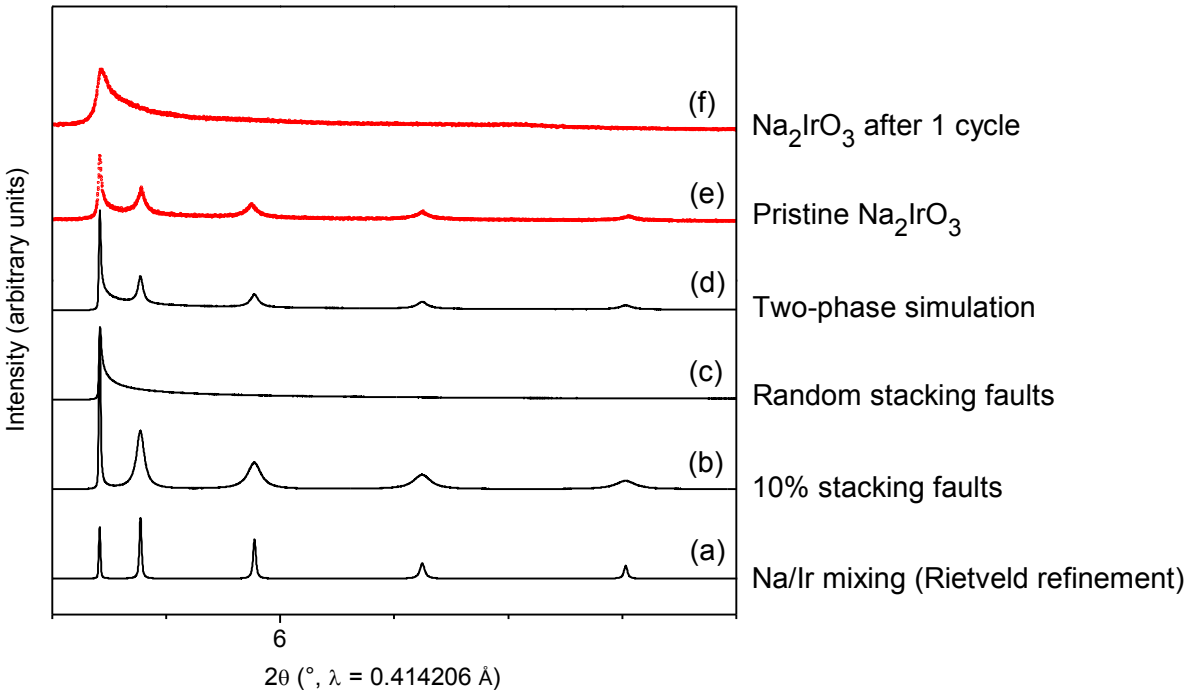

Fig. S3: Experimental superstructure peaks of the pristine and sample discharged after 1 cycle are compared to simulated superstructure peaks with different stacking models obtained using the FAULTS program. (a) Sharp peaks obtained from Ir/Na mixing in the honeycomb layers as obtained from Rietveld refinement. (b) Model with a 10% chance of changing the stacking direction of honeycomb layers, and 90% chance of conserving the same stacking direction as the previous one. (c) Random stacking of honeycomb layers. (d) Two-phase model alternating b and c descriptions with a 7:3 ratio. (e) Superstructure peaks of the pristine Na_2IrO_3 are in good agreement with the model d. (f) Superstructure peaks of the sample discharged after 1 cycle indicate a loss of ordering in the honeycomb stacking.

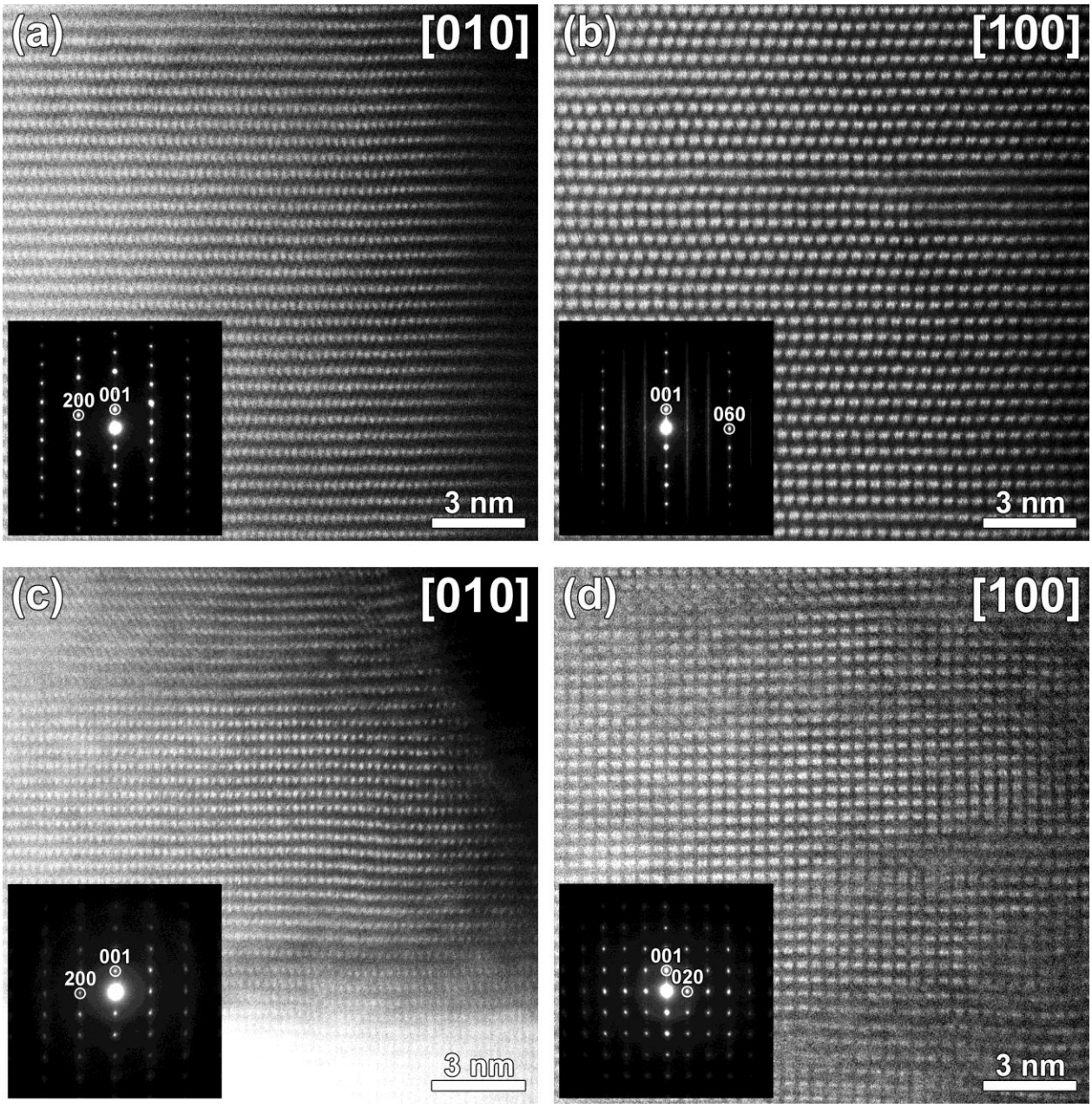

Fig. S4: TEM data for the sample after first charge-discharge cycle demonstrating that the material regains the O3 structure with well-ordered cubic close-packed O sublattice (a), but numerous stacking faults in the arrangement of the $NaIr_2$ honeycomb layers (b). Data for the discharged sample after 50 cycles demonstrating stabilization of the O1 structure even in the discharged state (c-d). Cation composition of the sample measured with EDX is Na/Ir = 0.55(11), which is only slightly higher than that for the charged sample (also after 50 cycles), i.e. Na/Ir = 0.44(8).

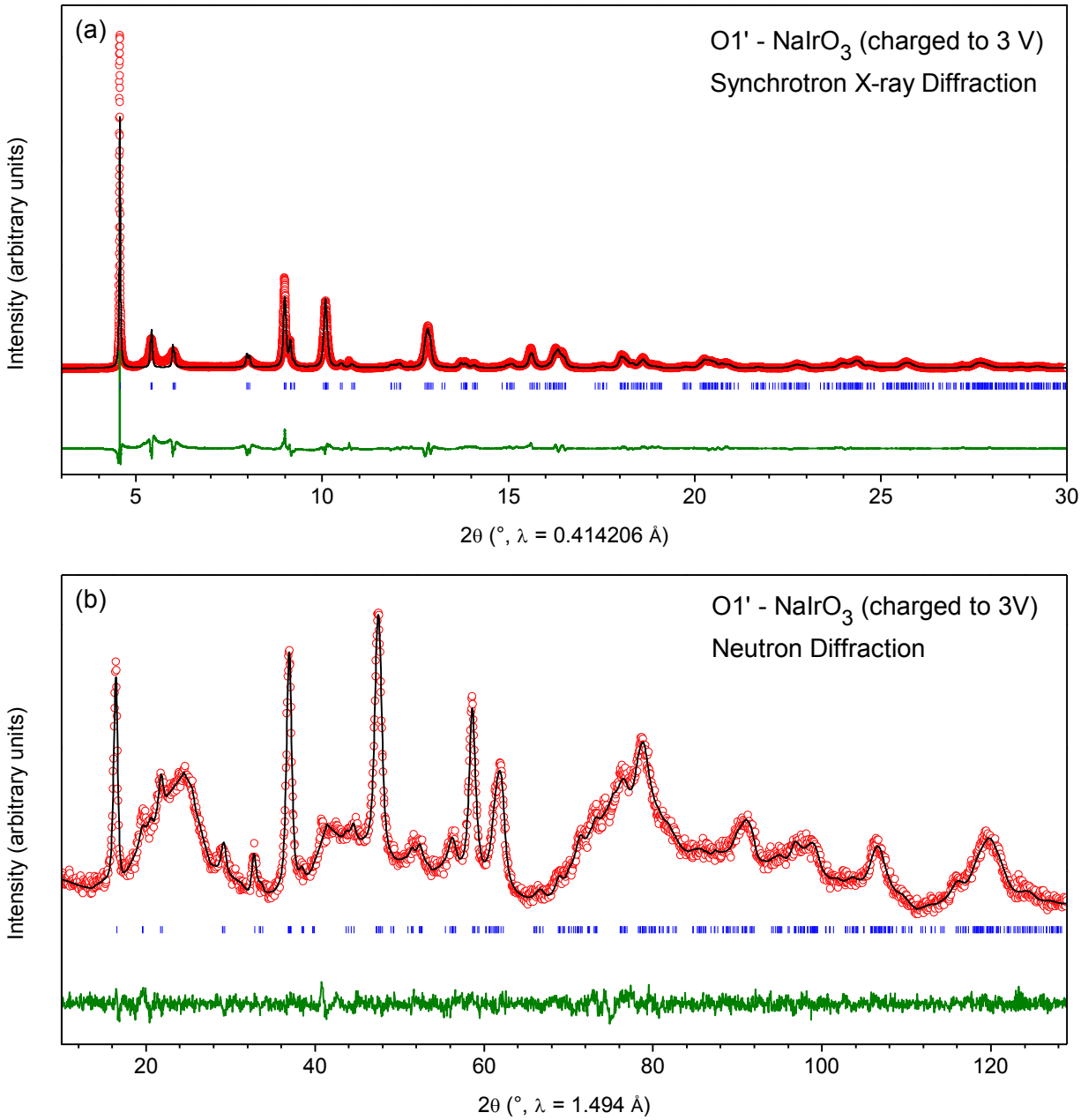

Fig. S5: Rietveld refinement of synchrotron X-ray (a) and neutron (b) diffraction patterns for $NaIrO_3$ (charged to 3V). The broad peaks in the neutron diffraction pattern come from the carbon mixed with Na_2IrO_3 to ensure electronic conductivity during cycling.

Table S2: Structural parameters for the O1'-$NaIrO_3$ sample. Atomic positions were refined from ND data and used as such for the refinement of SXRD data. Some mixing between Ir and Na sites in the honeycomb layer was allowed to artificially reduce the impact of stacking faults on the refinement.

O1' - $NaIrO_3$ (3V)

Space group : $P\bar{1}$

	a (Å)	b (Å)	c (Å)	α (°)	β (°)	γ (°)
SXRD	5.2887(3)	5.2809(2)	6.0323(3)	115.662(7)	90.597(8)	119.935(3)
ND	5.2912(7)	5.2841(7)	6.0468(8)	115.840(15)	90.479(12)	120.068(14)

Atom	Site	x	y	z	Occupancy	B (Å^2)
O1	2i	0.132(4)	0.521(6)	0.212(4)	1	0.37(14)
O2	2i	0.700(3)	0.722(3)	0.182(3)	1	0.37(14)
O3	2i	0.430(4)	0.159(5)	0.216(4)	1	0.37(14)
Na1	1a	0	0	0	0	0.115(14)
Ir1	1a	0	0	0	0.322(1)	0.115(14)
Ir2	2i	0.349(3)	0.677(3)	-0.011(2)	0.839(1)	0.115(14)
Na2	2i	0.868(3)	0.733(6)	0.5944(16)	1	2.33(17)
Na3	1f	0.5	0	0.5	0	N/A

Reliability parameters : χ^2 = 36.1, Bragg R-factor = 16.8 % (SXRD)
χ^2 = 1.50, Bragg R-factor = 1.50 % (ND)

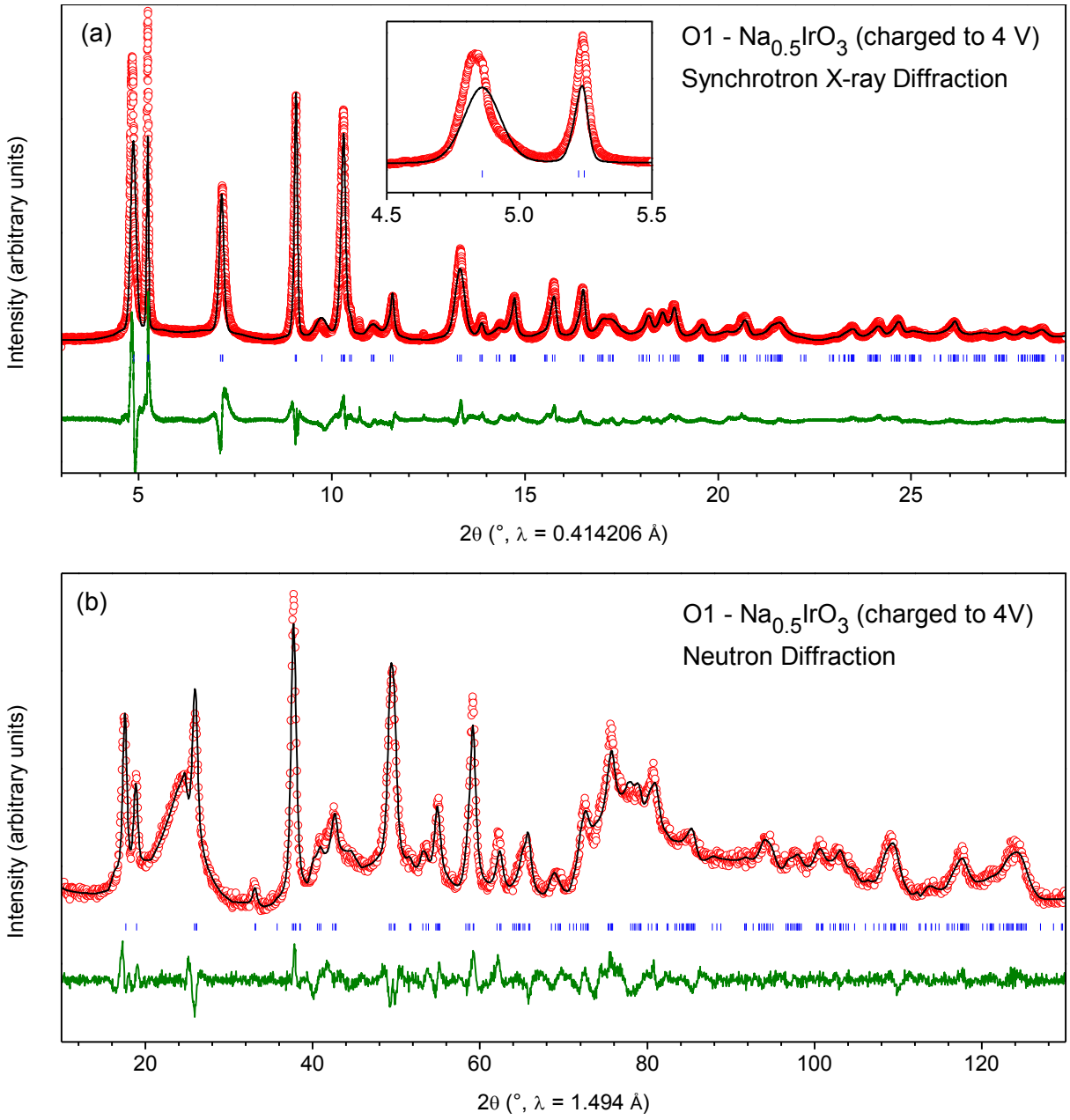

Fig. S6: Rietveld refinement of synchrotron X-ray (a) and neutron (b) diffraction patterns for the fully charged $Na_{0.5}IrO_3$ (4V). The inset highlights the unusual shape of the first peak, which prevents a good refinement of the data. The asymmetric broadening observed for this (001) peak suggests that the interlayer distances are not uniform in the material.

Table S3: Structural parameters for the O1-$Na_{0.5}IrO_3$ sample. Atomic positions were refined from ND data and used as such for the refinement of SXRD data.

O1 - $Na_{0.5}IrO_3$ (4V)

Space group : *C*2/*m*

	a (Å)	b (Å)	c (Å)	β (°)
SXRD	5.2534(2)	9.0633(2)	4.88271(19)	89.482(17)
ND	5.2457(5)	9.0657(9)	4.8707(4)	89.249(6)

Atom	Site	x	y	z	Occupancy	B (Å^2)
O1	8j	0.318(2)	0.3082(8)	0.7533(14)	1	3.72(19)
O2	4i	0.346(2)	0	0.8122(18)	1	2.3(2)
Ir1	4g	0	0.3339(13)	0	1	3.16(11)
Na1	2a	0	0	0	0	N/A
Na3	4h	0	0.33798	0.5	0	N.A
Na2	2c	0	0	0.5	1	0.77(19)

Reliability parameters : χ^2 = 6.45, Bragg R-factor = 4.39 % (SXRD)
χ^2 = 3.38, Bragg R-factor = 3.48 % (ND)

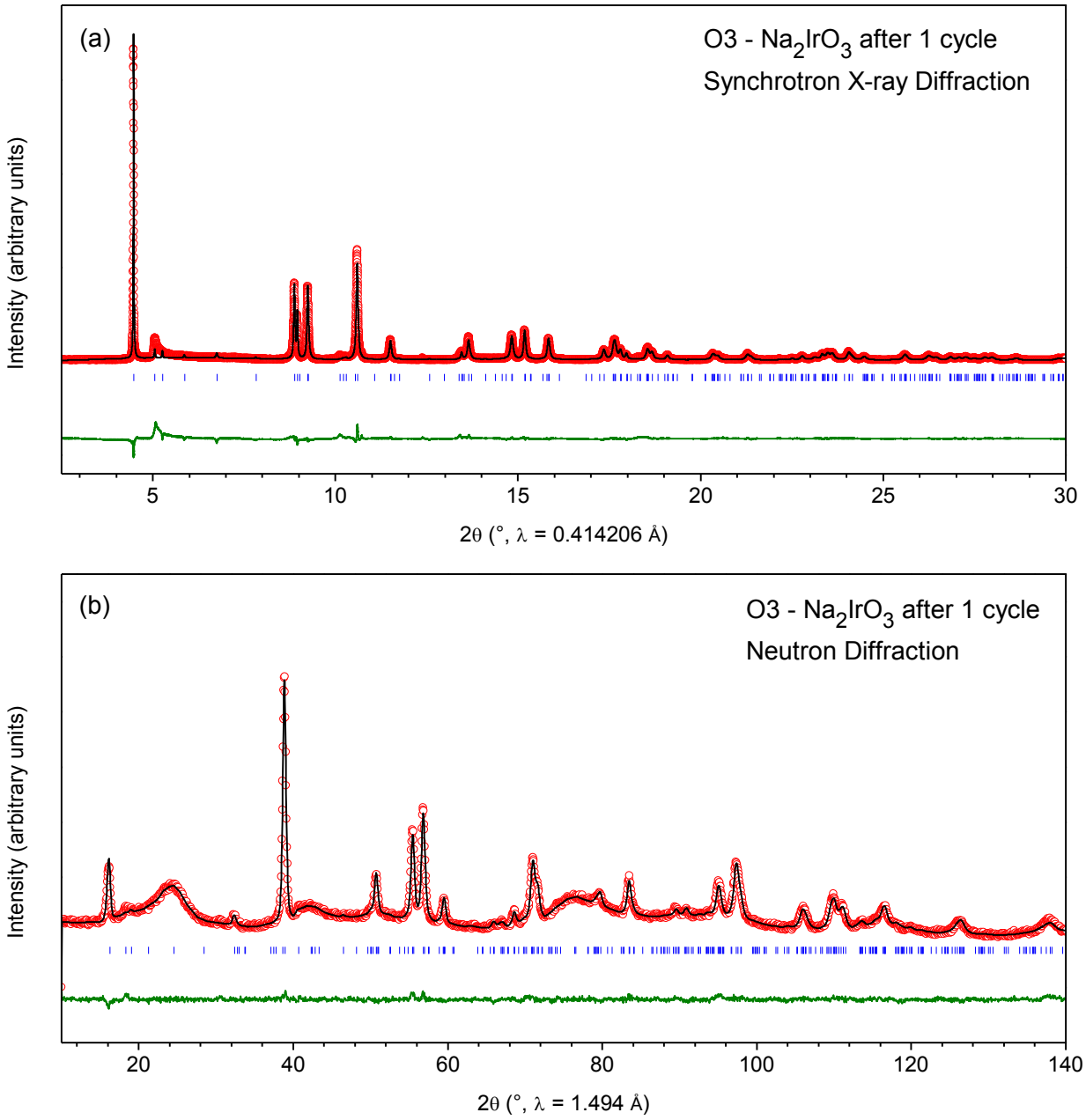

Fig. S7: Rietveld refinement of synchrotron X-ray (a) and neutron (b) diffraction patterns for Na_2IrO_3 after charging to 4 V and discharging to 1.5 V.

Table S4: Structural parameters for the Na_2IrO_3 sample after 1 cycle. Atomic positions were refined from ND data and used as such for the refinement of SXRD data. Some mixing between Ir and Na sites in the honeycomb layer was allowed to artificially reduce the impact of stacking faults on the refinement.

O3 - Na_2IrO_3 after 1 cycle

Space group : *C2/m*

	a (Å)	b (Å)	c (Å)	β (°)
SXRD	5.43086(5)	9.40476(16)	5.60504(5)	108.8291(8
ND	5.4427(2)	9.4033(5)	5.5999(2)	108.778(5)

Atom	Site	x	y	z	Occupancy	B (Å^2)
O1	8j	0.256(2)	0.3349(9)	0.7926(15)	1	2.81(13)
O2	4i	0.279(3)	0	0.803(3)	1	4.0(2)
Ir1	4g	0	0.3202(6)	0	0.874(8)	2.61(13)
Na1	4g	0	0.3202(6)	0	0.126(8)	2.61(13)
Na2	2a	0	0	0	0.748(8)	0.6(2)
Ir2	2a	0	0	0	0.252(8)	0.6(2)
Na3	4h	0	0.830(2)	0.5	1	3.1(4)
Na4	2d	0	0.5	0.5	1	3.7(5)

Reliability parameters : χ^2 = 10.4, Bragg R-factor = 11.8 % (SXRD)
χ^2 = 1.47, Bragg R-factor = 4.89 % (ND)

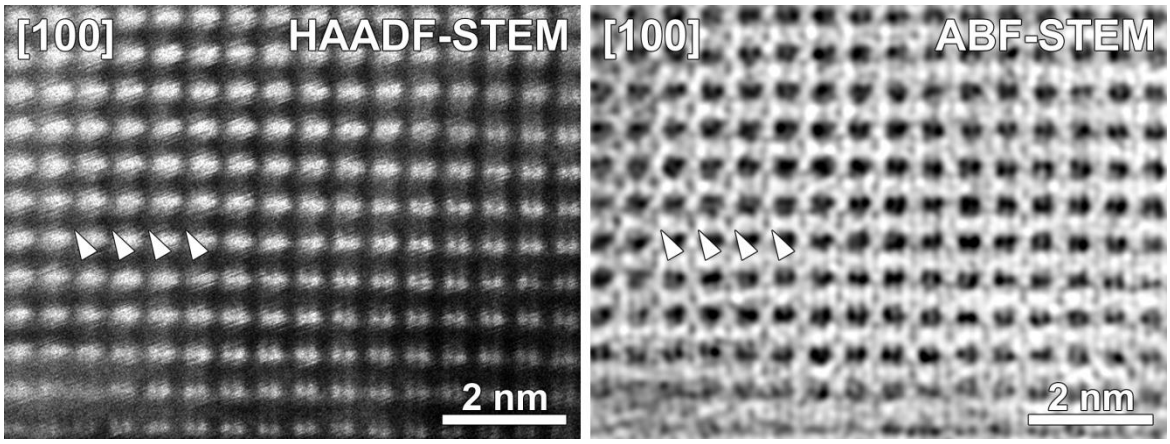

Fig. S8: Complementary HAADF-STEM and ABF-STEM images for the fully charged $Na_{0.5}IrO_3$ sample demonstrating that Na atoms in the structure primarily occupy positions between the empty octahedra of the honeycomb layers. Some Na columns are marked with arrowheads in the ABF-STEM image. They are not visible in the HAADF-STEM image ruling out the possibility of Ir migration in the Na layers.

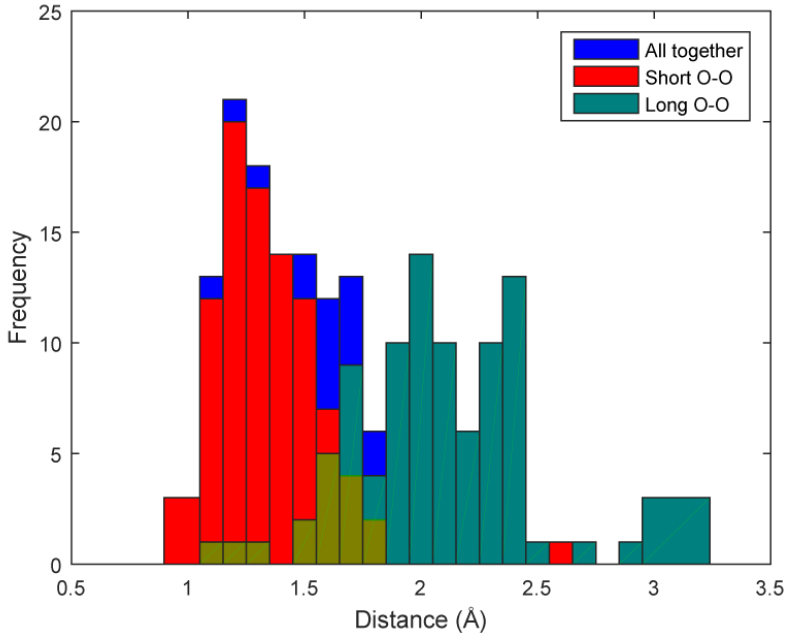

Fig. S9: Histograms of projected O-O distances measured from the [001] ABF-STEM image of fully charged $Na_{0.5}IrO_3$ structure. The histograms for short and long distances comprise 92 measured O-O separations, each. The average measured projected distances for short and long O-O distances are 1.33(3) Å and 2.07(4) Å, respectively.

Table S5: Structural parameters for the sample discharged after 50 cycles. 3 phases are present. Phase 1 was refined using the structural parameters of O3-Na_2IrO_3 after 1 cycle (Table S4) and complete mixing of Ir and Na sites in the honeycomb layer. Phase 2 corresponds to an Ir impurity. The remaining contribution of the pattern was fitted in pattern matching (Le Bail refinement) with a *C*2/*m* space group similar to that of the O1 structure.

Phase 1 : O3 - Na_2IrO_3 - Rietveld refinement

Space group : *C*2/*m*

	a (Å)	b (Å)	c (Å)	α (°)	β (°)	γ (°)
SXRD	5.42063(11)	9.40694(18)	5.61671(10)	90	109.0421(18)	90

Atom	Site	x	y	z	Occupancy	B (Å^2)
O1	8j	0.256(2)	0.3349(9)	0.7926(15)	1	1.0
O2	4i	0.279(3)	0	0.803(3)	1	1.0
Ir1	4g	0	0.3202(6)	0	2/3	1.0
Na1	4g	0	0.3202(6)	0	1/3	1.0
Na2	2a	0	0	0	1/3	1.0
Ir2	2a	0	0	0	2/3	1.0
Na3	4h	0	0.830(2)	0.5	1	1.0
Na4	2d	0	0.5	0.5	1	1.0

Phase 2 : Ir impurity - Rietveld refinement

Space group : $Fm\bar{3}m$

	a (Å)	b (Å)	c (Å)	α (°)	β (°)	γ (°)
SXRD	3.839	3.839	3.839	90	90	90

Atom	Site	x	y	z	Occupancy	B (Å^2)
Ir	4a	0	0	0	1	1.0

Phase 3 : O1* - Na_xIrO_3 - Pattern matching

Space group : *C*2/*m*

	a (Å)	b (Å)	c (Å)	α (°)	β (°)	γ (°)
SXRD	5.42839(11)	9.3664(2)	4.56187(7)	90	90.7332(17)	90

Reliability parameters : χ^2 = 1.11, Bragg R-factor = 1.63 % (Phase 1), 1.97 % (Phase 2), 0.224 % (Phase 3)

Table S6: Variation of cell parameters (in %) obtained from full structural relaxation with DFT and DFT-D3 compared with experimental values.

		Δa/a	Δb/b	Δc/c	Δα/α	Δβ/β	δγ/γ
Na_2IrO_3	DFT	2.14	0.06	0.41	0.00	0.51	0.00
	DFT D3	1.26	1.17	2.20	0.00	0.56	0.00
$NaIrO_3$	DFT	1.42	1.57	0.51	0.17	0.90	0.35
	DFTD3	0.91	1.05	1.61	0.10	1.13	0.17
$Na_{0.5}IrO_3$	DFT	0.88	1.17	2.87	0.00	0.85	0.00
	DFTD3	0.49	0.88	2.33	0.00	0.68	0.00

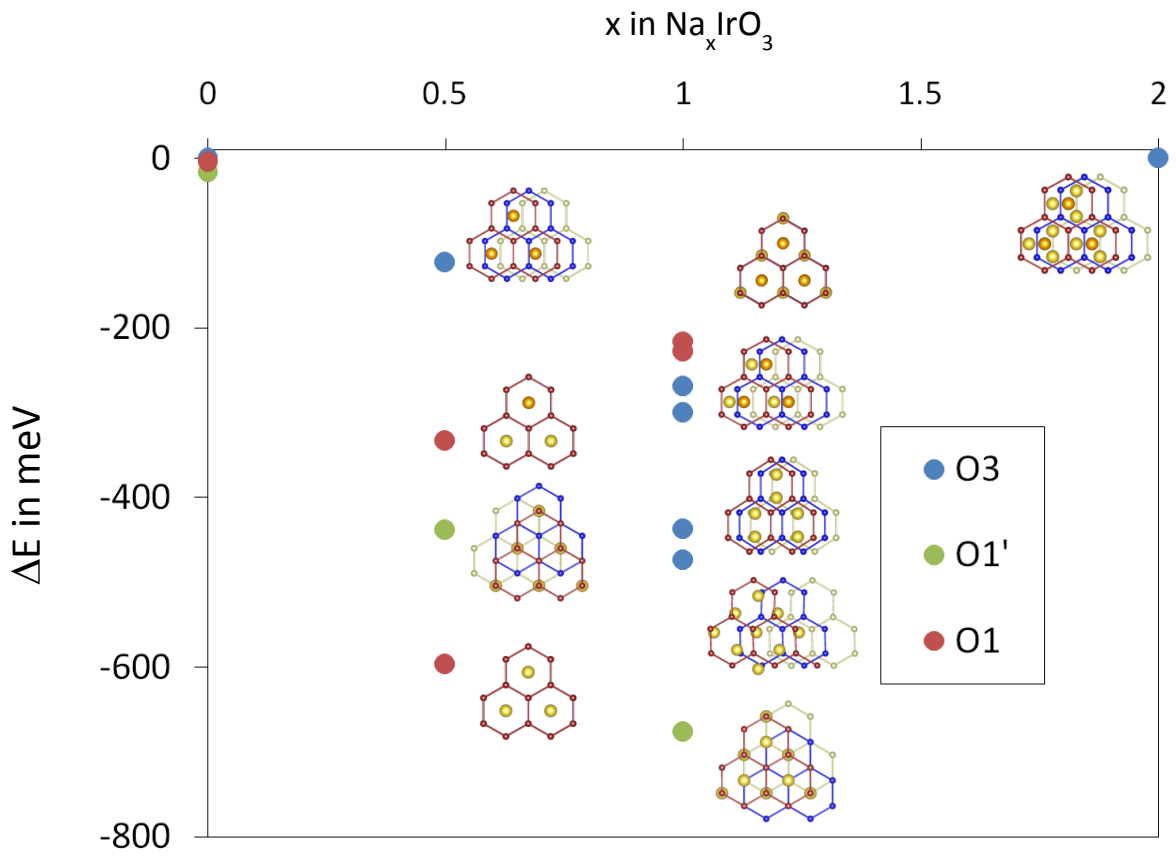

Figure S10. Phase stability diagrams of Na_2IrO_3 computed with DFT-D3 and considering the different polymorphs O3, O1' and O1. It confirms the stability of the polymorph O1' (O1) for the $NaIrO_3$ ($Na_{0.5}IrO_3$) compositions. Selected structural organization of the different polymorph are displayed, highlighting the different stacking of the $NaIr_2$ layer and the different position of Na. Yellow and orange atoms refers to sodium in the Na and $NaIr_2$ layers, respectively. It shows that polymorphs having sodium in the $NaIr_2$ layer are less stable than other for $x < 2$, suggesting that sodium in the $NaIr_2$ layered is removed first.

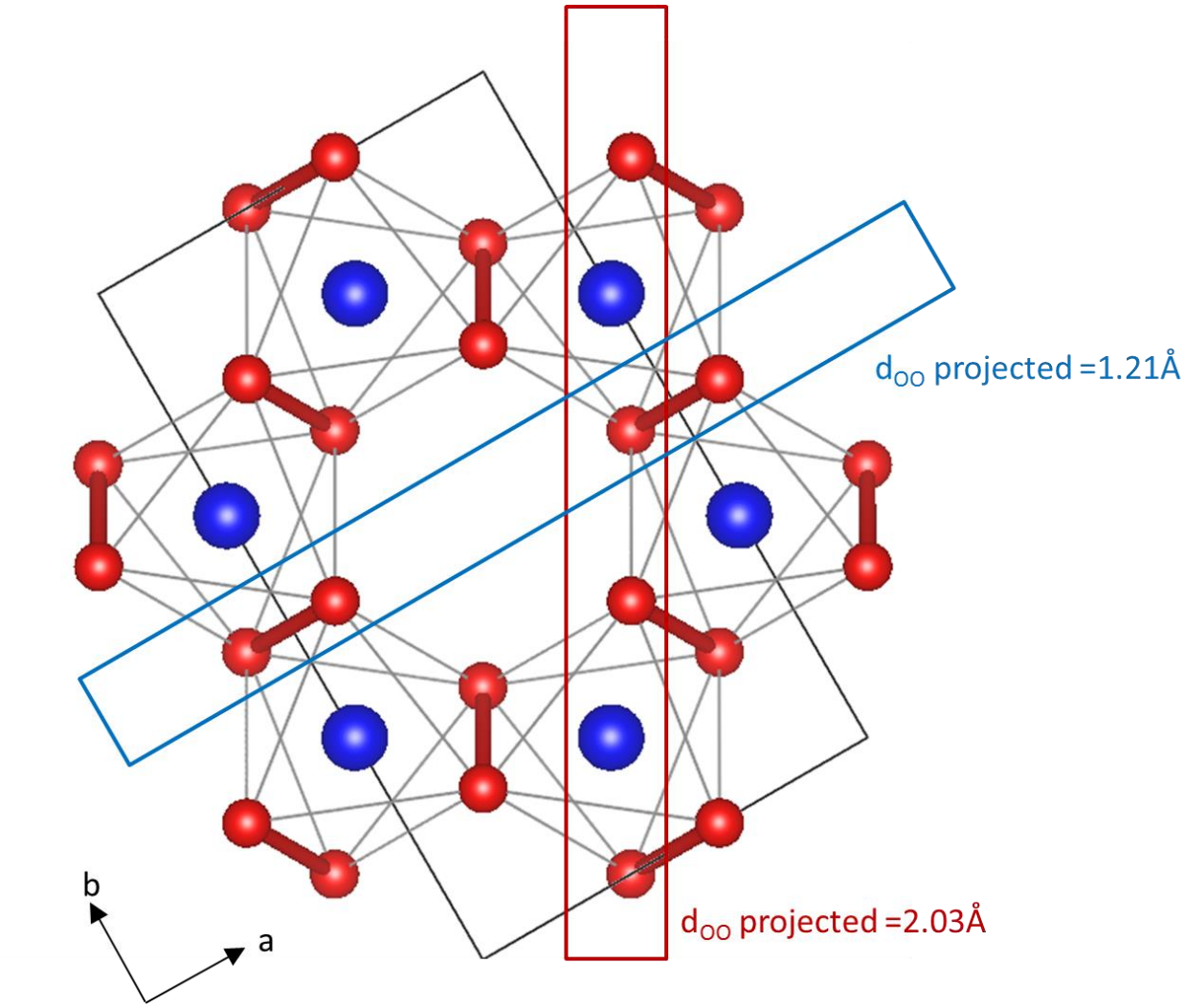

Figure S11: Crystal structure of $Na_{0.5}IrO_3$ as obtained with DFT-D3 and associated projected O-O distances.